

The Distribution of Vacua in Random Landscape Potentials

Low Lerh Feng, Shaun Hotchkiss and Richard Easther

Department of Physics,
University of Auckland,
Private Bag 92019,
Auckland, New Zealand

E-mail: lerh.low@auckland.ac.nz, s.hotchkiss@auckland.ac.nz,
r.easther@auckland.ac.nz

Abstract. Landscape cosmology posits the existence of a convoluted, multidimensional, scalar potential – the eponymous “landscape” – with vast numbers of metastable minima. The huge number of minima supported by landscape potentials motivate arguments that landscape cosmology reduces tuning problems associated with a small but non-zero vacuum energy to issues of anthropic or “environmental” selection. The properties of random matrices and random functions in many dimensions have been used to investigate conceptual issues associated with landscape scenarios; in this paper we explore the distribution of minima as a function of vacuum energy in an N -dimensional Gaussian random potential. We derive a “likelihood” function for the density of minima in N dimensions, showing that after rescalings its properties are fully defined by the dimensionality and a single free parameter. We present a mix of analytical and numerical results at low N and extrapolate these to larger values of N , extracting estimates for $P(\Lambda)$, the distribution function of vacuum energies in these scenarios. [\[RE: maybe one more sentence\]](#)

Contents

1	Introduction	1
2	Random Potentials in N Dimensions	3
3	Peak Probabilities: F and N	6
3.1	Landscape Heuristics	7
3.2	$N \leq 10$: Direct Evaluation of $P(\Lambda)$	8
3.3	Gaussian Approximations to the Integral	9
4	Implications for Multiverse Cosmology	10
5	Conclusion	10
6	Appendix	12
6.1	Density of peaks for $N = 4$	12
6.2	$p(F s.p.)$ for $N = 2$	12

1 Introduction

Over the last two decades cosmology has developed in apparently paradoxical directions. Observationally, the much-heralded rise of “precision cosmology” makes it possible to measure key parameters to within a few percent, setting stringent tests for the detailed evolutionary narrative provided by concordance Λ CDM cosmology [1, 2]. Conversely, theoretical investigations of both slow-roll inflation and string theory along with the information that the dark energy density is non-zero motivates for the theoretical investigation of multiverse-like scenarios. In particular, studies of stochastic inflation [3, 4] suggest that the mechanism that produces astrophysical density perturbations could also support *eternal inflation*, generating infinite numbers of *pocket universes* [5]. Likewise, studies of flux compactified string vacua points to a possible *landscape* [6] or *discretuum* [7] of vacua within the theory. These developments, together with the non-zero vacuum energy density, open the door to anthropic explanations of its value, insofar as a value that was exactly zero could be suggestive of an underlying symmetry.

Stochastic (or eternal) inflation on its own implies the existence of an multiverse composed of many pocket universes, but this does not require that the “low energy” (i.e. LHC scale) physics or vacuum energy differs between pockets: for example, naive quadratic inflation model is potentially eternal, but has a unique vacuum. Landscape hypotheses posit the existence of multiple vacua which can, in principle, be populated by stochastic inflation. The best known of these is the string landscape, built on the plethora of flux-stabilised vacua that exist inside Calabi-Yau spaces, but it is not necessarily the unique realisation of this scenario. The complexity of the landscape

and the vast number of vacua it supports is the basis of its purported explanatory power: the number of vacua is almost uncountably large (e.g. 10^{500} or greater [42]) so almost any value of the vacuum energy can conceivably be realised within it.

The detailed properties of the landscape are almost entirely unknown – it is still unclear whether any specific stringy construction realises the $SU(3) \times SU(2) \times U(1)$ gauge group of the Standard Model. More recently the Swampland Conjecture suggests that all stable minima of the theory might actually be “underwater” [8], located at negative values of Λ . If true, this would require that the cosmological dark energy was underpinned by dynamical quintessence-like evolution.

An alternative route to understanding landscape scenarios is to strip them down to their barest essence – the proposal that multiverse cosmology is realised within a *random* multidimensional ($N \sim 100$ or more) potential of interacting scalar fields.¹ In this approach the apparent complexity of a multidimensional landscape provides leverage to develop an understanding of its properties. The first steps in this direction were taken by Aazami and Easther [12], investigating ensembles of Hessian matrices describing extrema in a random landscape. At a minimum in the landscape the eigenvalues of the Hessian are all positive. For simple random matrix distributions eigenvalues are likely to be evenly distributed between positive and negative values with fluctuations away from this situation being strongly suppressed at even moderate values of N , suggesting that the number of minima is super-exponentially smaller than the number of saddles. This simple argument is substantially modified when it is noted that the individual entries of the Hessians matrices of random functions are correlated and are thus not drawn from identical, independent distributions, a common premise in random matrix theory [32][35]. This overall approach has been pursued and extended in a number of directions [14–21].

This line of enquiry has also provided motivation for more general studies of the properties of random matrices and random functions at large N . [13, 29–34] The topic is of interest to multiple fields, including statistical mechanics, string theory, and complex dynamics. [22–28]

In conventional inflationary scenarios, accelerated expansion occurs when the gradient of the potential is small (so-called “slow-roll”), and trajectories typically end in one of the potential’s minima. If this is the global minimum, the end-state is stable. However, from a local minimum, bubbles of space can tunnel to lower-lying vacua, rendering local minima are metastable, although often with lifetimes much greater than the age of the universe. Yamada and Vilenkin [21] investigate the distribution of eigenvalues at stationary points as well as the probability of minima given stationary points, deriving the probability that a given extremum is a minimum (as opposed to a saddle) as a function of the potential value, where as our goal here is to investigate $P(\Lambda)$. In particular, we show that for some region of parameter space that a potential with 10^M minima (where M is a number of order $\mathcal{O}(100)$), $P(\Lambda > 0) < 10^{-M}$, so that it is conceivable that these scenarios could not provide solutions with a metastable,

¹Random is used here in the context of random function theory [9–11]. We refer to random functions rather than random fields, the nomenclature often seen in the mathematical literature, to avoid confusion with the individual scalar fields that are coupled by the potential.

positive vacuum energy. More generally, these considerations may be used to establish a weakly non-uniform measure on the vacuum energy.

We proceed from a generalisation of the Kac-Rice formalism [36, 37] and the machinery developed by Bond, Bardeen, Kaiser and Szalay [38] for studying the statistics of Gaussian random fields in the context of cosmological perturbation theory to N dimensions. We give exact results for small N , directly evaluate numerical integrals for moderate N and then extrapolate these results to larger values of N . We find that the results depend on just one free parameter σ_2 which can be computed directly from the power spectrum and then discuss the implications of these results for landscape cosmology and notions of anthropic selection.

2 Random Potentials in N Dimensions

We begin by developing an N -dimensional analogue of the treatment of three dimensional random functions due to Bardeen, Bond, Kaiser and Szalay (henceforth BBKS) [38], generalising their derivation and keeping their notation as far as possible. An N -dimensional scalar-valued function $F(r)$ is a set of values that fill each point of N -dimensional space. The function is *random* if its values depend on a probability distribution function,

$$P[F(r_1), F(r_2), \dots, F(r_m)] dF(r_1) dF(r_2) \dots dF(r_m) \quad (2.1)$$

where r_i is a position in N dimensional space. This corresponds to the probability that the function takes value $F(r_1) \pm dF(r_1)$ at position r_1 , $F(r_2) \pm dF(r_2)$ at position r_2 , and so on. The function is *Gaussian random* if the probability distribution function is an N -dimensional Gaussian function,

$$P(y_1, \dots, y_N) dy_1 \dots dy_N = \frac{e^{-Q}}{[(2\pi)^N \det(M)]^{1/2}} dy_1 \dots dy_N, \quad (2.2)$$

$$Q \equiv \frac{1}{2} \sum \Delta y_i (M^{-1})_{ij} \Delta y_{ij}.$$

Here M is the *covariance matrix*,

$$M_{ij} \equiv \langle \Delta y_i \Delta y_j \rangle \quad (2.3)$$

while Δy_i is the difference between the measured value and the average, $\Delta y_i \equiv y_i - \langle y_i \rangle$. For a Gaussian random function, the probability distribution only depends on M , which in turn only depends on the two-point correlation function $\langle \Delta y_i \Delta y_j \rangle$. In other words, the two-point correlation function completely determines the statistical properties of the Gaussian random function.

In our application, the function value we're interested in is the potential of the landscape ϕ , so henceforth we will replace y with F . [RE: would this be clearer to say the the independent variables were ϕ and the function / potential V ?][LL: We're using F because that's the symbol used by BBKS] The two-point correlation function is, by definition, the Fourier transform of the power spectrum $P(k)$,

$$\langle F_\alpha(\vec{x}) F_\beta(\vec{y}) \rangle = \frac{\delta_{\alpha\beta}}{(2\pi)^N} \int d^N k e^{i\vec{k} \cdot (\vec{x} - \vec{y})} P(k) \quad (2.4)$$

where \vec{x} and \vec{y} are directional vectors, while α and β are labels for the different functions. We define moments of the power spectrum by

$$\sigma_n^2 = \frac{1}{(2\pi)^N} \int d^N k (k^2)^n P(k) \quad (2.5)$$

i.e. $\langle F_\alpha F_\beta \rangle = \sigma_0^2 \delta_{\alpha\beta}$. We can differentiate Eq. 2.5 to get

$$\begin{aligned} \langle \eta_{\alpha,i}(\vec{x}) \eta_{\beta,j}(\vec{x}) \rangle &= \frac{\delta_{\alpha\beta}}{(2\pi)^N} \frac{\partial}{\partial x^i} \frac{\partial}{\partial y^j} \int d^N k e^{i\vec{k} \cdot (\vec{x} - \vec{y})} P(k) \Big|_{\vec{y}=\vec{x}} \\ &= \frac{\delta_{\alpha\beta}}{(2\pi)^N} \int d^N k k^i k^j P(k) \end{aligned}$$

where $\eta_{\alpha,i}$ indicates the derivative of $F_\alpha(\vec{x})$ with respect to x^i . Because of spherical symmetry, we know that the right hand side is proportional to δ_{ij} . Therefore

$$\begin{aligned} \langle \eta_{\alpha,i} \eta_{\beta,j} \rangle &= K \delta_{\alpha,\beta} \delta_{ij} \rightarrow \delta_{ij} \langle \eta_{\alpha,i} \eta_{\beta,j} \rangle = N K \delta_{\alpha,\beta} = \sigma_1^2 \\ &\rightarrow K = \frac{1}{N} \sigma_1^2 \end{aligned}$$

[RE: missing comma on the LHS above??] [LL: No missing comma (same notation as BBKS Eq. A1)] A similar analysis holds for the second derivatives ξ_{ij} , and the resulting relations between the various moments of the power spectrum, the function values, and the derivatives are:

$$\begin{aligned} \langle FF \rangle &= \sigma_0^2 \\ \langle \eta_i \eta_j \rangle &= \frac{1}{N} \delta_{ij} \sigma_1^2 \\ \langle \phi \eta_{ij} \rangle &= -\frac{1}{N} \delta_{ij} \sigma_1^2 \\ \langle \xi_{ij} \xi_{kl} \rangle &= \frac{1}{N(N+2)} \sigma_2^2 (\delta_{ij} \delta_{kl} + \delta_{il} \delta_{jk} + \delta_{ik} \delta_{jl}) \end{aligned} \quad (2.6)$$

For $N = 3$ this reduces to BBKS's equation A1.

We define the following vector:

$$\alpha_i = \{F, \eta_1, \eta_2, \dots, \xi_{11}, \xi_{22}, \dots, \xi_{NN}, \xi_{N-1,N}, \xi_{N-2,N}, \dots, \xi_{1N}, \xi_{N-2,N-1}, \dots, \xi_{1,N-1}, \dots, \xi_{12}\} \quad (2.7)$$

The subscript i serves only as an identifier for the element of the vector (e.g. $\alpha_1 = F$) and has no other meaning. With this choice for α (equivalent to Δy in Eq. 2.2), the

covariance matrix $M_{ij} \equiv \langle \alpha_i \alpha_j \rangle$ and its inverse $K \equiv M^{-1}$ takes the following general form:

$$\begin{aligned}
K_{\phi,\phi} &= \frac{\sigma_2^2}{\sigma_0^2 \sigma_2^2 - \sigma_1^4} \\
K_{\phi,\xi_{ij}} &= \frac{\sigma_1^2}{\sigma_0^2 \sigma_2^2 - \sigma_1^4} \\
K_{\eta_i,\eta_j} &= \frac{N}{\sigma_1^2} \\
K_{\xi_{ii},\xi_{ii}} &= \frac{N(N+2)}{\sigma_2^2} \\
K_{\xi_{ij},\xi_{ij}} &= \frac{N\sigma_0^2 \sigma_2^2 - (N+2)\sigma_1^4}{2(\sigma_1^4 \sigma_2^2 - \sigma_0^2 \sigma_2^4)}, (i \neq j) \\
K_{\xi_{ii},\xi_{jj}} &= \frac{(N(N+1) - 2)\sigma_1^4 - N(N+1)\sigma_0^2 \sigma_2^2}{2(\sigma_1^4 \sigma_2^2 - \sigma_0^2 \sigma_2^4)}, (i \neq j)
\end{aligned}$$

and all other terms are zero. The probability distribution of α_i is, from Eq. 2.2

$$p(\alpha_i) = \frac{1}{(2\pi)^{N/2} \sqrt{\det M}} e^{-\frac{1}{2} \alpha K \alpha} \quad (2.8)$$

We can usually ignore the constant prefactor since we will primarily be concerned with ratios of probabilities. We begin work in the basis

$$\begin{aligned}
\sigma_2 x_1 &= -\nabla^2 \phi = -(\xi_{11} + \xi_{22} + \dots + \xi_{NN}) \\
\sigma_2 x_2 &= -(\xi_{11} - \xi_{22}) \\
\sigma_2 x_3 &= -(\xi_{11} + \xi_{22} - 2\xi_{33}) \\
\sigma_2 x_4 &= -(\xi_{11} + \xi_{22} + \xi_{33} - 3\xi_{44}) \\
&\dots
\end{aligned}$$

x_1, x_2, x_3, \dots are analogous to BBKS's x, y, z . Following BBKS, we introduce $\nu = F/\sigma_0$. With this choice of basis, the nonzero correlations are (from Eq. 2.6):

$$\langle \nu^2 \rangle = 1, \langle x_1^2 \rangle = 1, \langle x_2^2 \rangle = \langle \xi_{11}^2 - 2\xi_{11}\xi_{22} + \xi_{11}^2 \rangle = \frac{4}{N(N+2)} \quad (2.9)$$

$$\langle x_3^2 \rangle = \frac{12}{N(N+2)}, \dots, \langle x_n^2 \rangle = \frac{2n(n-1)}{N(N+2)}. \quad (2.10)$$

The factor $\alpha K \alpha$ (Q in BBKS) in Eq. 2.8 takes the form

$$\begin{aligned}
2Q &= \nu^2 + \frac{(x_1 - x_*)^2}{1 - \gamma^2} + \frac{N(N+2)}{4} x_2^2 + \frac{N(N+2)}{12} x_3^2 + \dots + \frac{N(N+2)}{2n(n-1)} x_n^2 \\
&\quad + \frac{N \boldsymbol{\eta} \cdot \boldsymbol{\eta}}{\sigma_1^2} + \sum_{i,j;i>j}^N \frac{N(N+2)\xi_{ij}}{\sigma_2^2}
\end{aligned} \quad (2.11)$$

where $x_* \equiv \gamma\nu$ and $\gamma = \frac{\sigma_1^2}{\sigma_2\sigma_0}$. This is the equivalent of BBKS Eq. (A4) for N -dimensions. Note the first two terms remain constant for all N , but the remaining terms vary. The η terms are zero at minima by definition, while the off-diagonal ξ_{ij} terms can be Euler-rotated away by choosing an appropriate set of axes. The ξ matrix is already symmetric (by rotational symmetry), and Euler rotation turns it diagonal.[39] The upshot is that the symmetric ξ matrix becomes a diagonal matrix where the individual elements are the eigenvalues $\lambda_i = -\xi_{ii}$ of the Hessian. We are interested in minima, hence we demand all second derivatives to be positive, i.e. all eigenvalues to be positive.² From here, the analysis is exactly the same as BBKS, except that when we define the ordering of the eigenvalues $\lambda_1 \geq \lambda_2 \geq \lambda_3 \dots \geq 0$, our boundary conditions become $x_1 \geq x_N \geq x_{N-1} \dots \geq x_2 \geq 0$ because of the different choice of basis. This leads to significantly simpler boundary conditions, for example in 3D our conditions are $x_2 \geq 0, x_2 \leq x_3$, and $x_1 \geq x_3$ (compare BBKS's equation between Eq. (A14) and Eq. (A15)).

This yields the following expression for the density of peaks

$$N = A \int_{\lambda_1 \geq \lambda_2 \geq \lambda_3 \dots \geq 0} F \times e^{-Q} d\nu dx dy dz \dots \quad (2.12)$$

where F has the form

$$F = \left(\prod_i^N \lambda_i \right) \left(\prod_{i < j} |\lambda_i - \lambda_j| \right), \quad (2.13)$$

Q is given by Eq. 2.11, A is some constant factor, and the integration limits are only over the region where the conditions are satisfied.

[RE: this above is going to need to be checked for self-consistency and trimmed]

[RE: can trim / compress/ move this At this point we will briefly discuss the results obtained by Yamada and Vilenkin [21]. They have derived $p(\min|U, s.p.)$, while we are interested in $p(F > 0|\min) = \int_0^\infty p(F|\min)dF / \int_{-\infty}^\infty p(F|\min)dF$. The two are related by $p(F|\min) = \frac{p(\min|F, s.p.)p(F|s.p.)}{p(\min|sp)}$.³The numerator is independent of F , so it cancels. Therefore the two probabilities can be related with knowledge of $p(F|s.p.)$. However, this quantity is not trivial to compute. We have been able to derive an analytical formula for this in 2D (see appendix), but even in 2D the complexity is formidable.]

3 Peak Probabilities: F and N

Our overall goal here is to understand the form $P(\Lambda)$ for Gaussian random landscape potentials, the probability distribution that defines the distribution of vacuum energies at minima in the landscape. The overall probability Eq. 2.12 depends on the value of

²Note there is an alternative convention where all eigenvalues being *negative* corresponds to maxima. Although it can be confusing, it is a simple matter to convert results from one convention to the other; $p(\min)$ is simply $1 - p(\max)$.

³This result is derived using Bayes theorem, as well as the fact that minima are necessarily stationary points

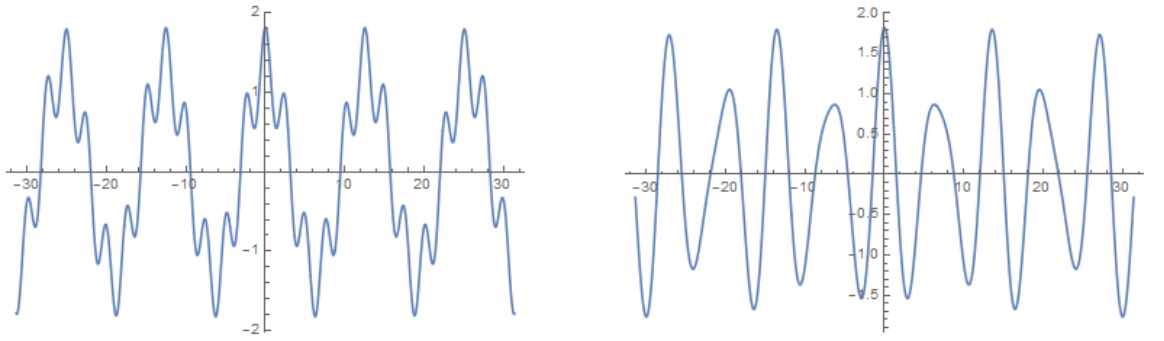


Figure 1. We show illustrative realisations of 1D functions. The left case has a larger second moment and more “short scale” power, allowing minima (maxima) to appear in significant numbers above (below) zero. When γ is close to unity the spectrum is dominated by longer wavelength modes, and most minima are low-lying.

F and the moments of the power spectrum σ_0, σ_1 , and σ_2 . Since we will focus on a purely Gaussian landscape with no physical parameters that set a scale we can work with both σ_0 and σ_1 equal to unity. The former is achieved by setting the average value of F to unity by an additive rescaling, as can be seen from Eq. 2.6, and therefore $F = \nu$. Likewise, σ_1 responds to the average magnitude of the first derivatives and can be set to unity by rescaling the units of length, leaving σ_2 as the only nontrivial parameter. It can be shown that if $\sigma_0 = \sigma_1 = 1$, $\sigma_2 > 1$,⁴ in much of what follows we parameterise the landscape by $\gamma = 1/\sigma_2$ [RE: should we actually show this; I know you sorted this out] [LL: I think we cite Yamada & Vilenkin for this and leave out the explicit proof] and the dimensionality N , in the knowledge that $0 < \gamma < 1$.

The probability P gives the (relative) likelihood of finding a minimum [RE: at what point do we start talking about minima, not maxima; we should probably flip it from the start] [LL: I don’t understand, we’ve been using minimum since the beginning?] with value V and the given values of x_i which will, in turn, determine the eigenvalues of the Hessian at the minimum. Up to an undetermined overall constant the probability of obtaining a peak with value F is given thus given by

$$P(V) = \int dx_1 \cdots dx_N F(x) \exp(-Q) \quad (3.1)$$

where it is assumed that all such integrals are over $x_1 \geq x_N \geq x_{N-1} \dots \geq x_2 \geq 0$.

3.1 Landscape Heuristics

We begin by making a qualitative exploration of the properties of the landscape. From a purely computational perspective, the F term complicates what would otherwise be a relatively simple Gaussian function. However, note that the integrand vanishes when any two “adjacent” λ_i become equal, enforcing an “eigenvalue repulsion” in the Hessian matrices for the maxima and minima.

⁴Per Ref. [21], if $\sigma_0 \sigma_2 - \sigma_1^2 < 0$, then the probability distribution Eq. 2.8 cannot be normalized.

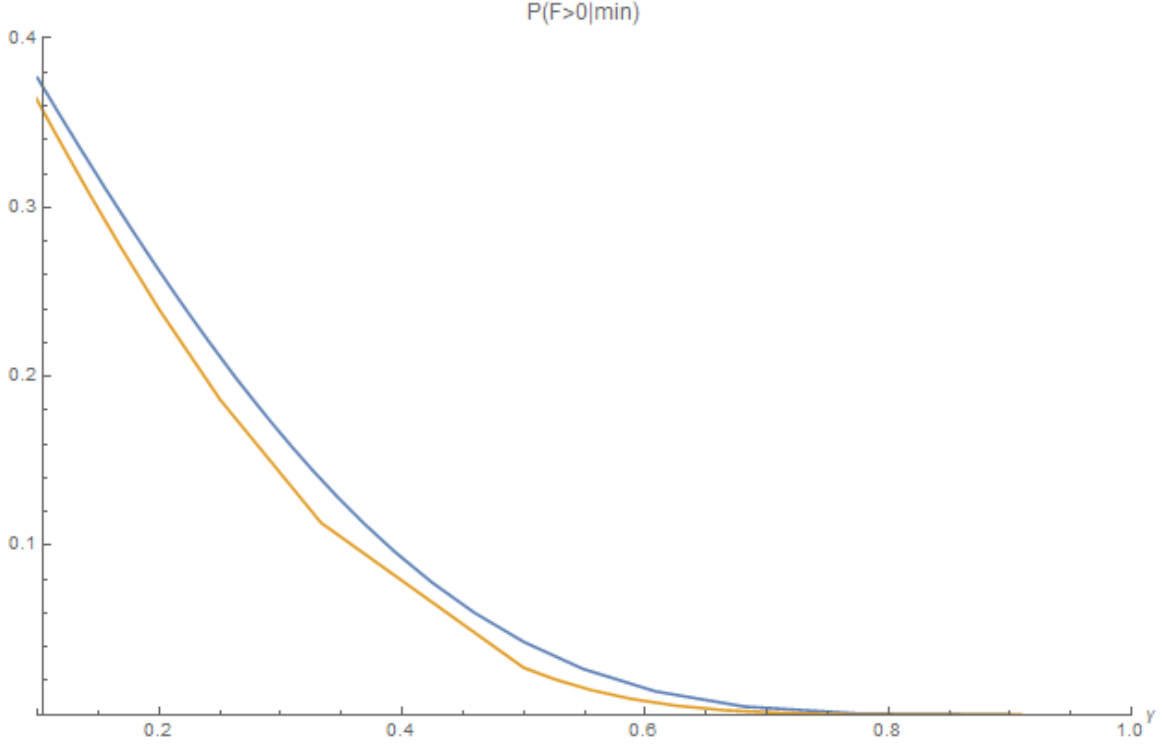


Figure 2. The probability that a given minimum has $F > 0$ as a function of γ , for $N = 5, 6$ (blue and orange lines respectively). The probability for $N = 5$ is always larger than that for $N = 6$.

Here, we are interested in $P(F)$; looking at Eq. 2.11 we see that if γ is close to unity, the first term will dominate, heavily penalising negative values of F . [RE: again we will need to sort our labeling, and whether we follow BBKS and talk about maxima, or switch to minima all the way through] Figure 1 shows two illustrative examples; at larger values of γ the power spectrum is effectively “red” and the overall function is dominated by longer wavelength modes. By contrast, when γ is small the spectrum is “blue” and dominated by shorter wavelengths, making it more likely that both kinds of extrema can be found on either side of zero. Conversely, as N increases the summation in Q will typically grow, making it less likely to find minima and maxima on the “wrong” side of zero.

Consequently, we can develop the expectation that for large N (e.g. $\mathcal{O}(100)$) a Gaussian random landscape potential will have $P(\Lambda)$ such that $\Lambda < 0$ is strongly favoured over positive values. Beyond this, given knowledge of the power spectrum and thus γ we will be able to draw detailed inferences about the form of $P(\Lambda)$.

3.2 $N \leq 10$: Direct Evaluation of $P(\Lambda)$

For relatively small values of N we can directly integrate over the x_i to numerically evaluate $P(\Lambda)$ without any further approximations in a numerical algebra package; and for $N \leq 10$ the VEGAS [40] Monte Carlo integration routine in the GNU Scientific

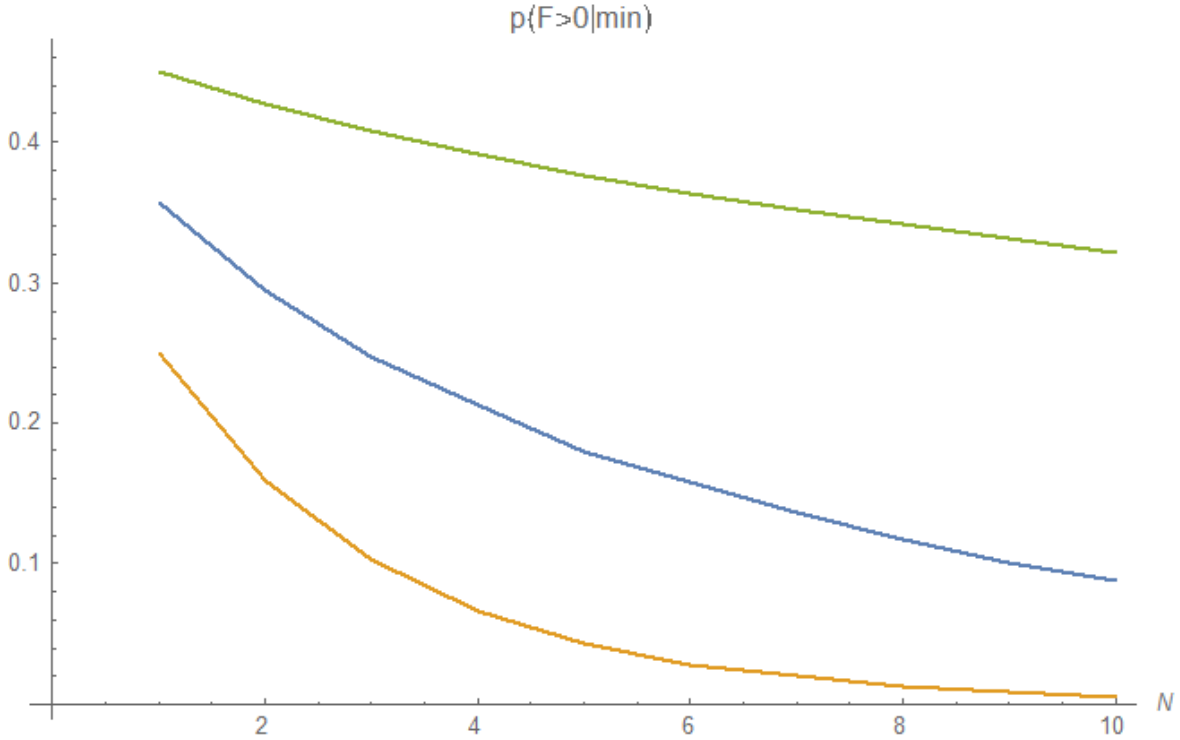


Figure 3. A plot showing the value of $P(F > 0|min)$ as a function of N with $N \leq 10$, for γ values $\frac{1}{5}$, $\frac{1}{3.5}$ and $\frac{1}{2}$ from top to bottom.

Library.[41] gives results to several figures. In order to characterise the landscape, consider

$$P_{\pm} = \frac{\int_0^{\infty} d\Lambda P(\Lambda)}{\int_{-\infty}^{\infty} d\Lambda P(\Lambda)} \quad (3.2)$$

which is a measure of the fraction of minima lying “above the waterline”, or at positive values of the effective vacuum energy.

In Fig. 2, we present P_{\pm} ; as expected, if the potential is highly oscillatory with σ_2 is large, or small γ is small, P_{\pm} tends towards 0.5 – an equal likelihood of any given extremum being a maximum or a minimum. Conversely, if the potential is very smooth (σ_2 is small; γ is close to unity), P_{\pm} tends towards 0. Moreover, for any given γ , the P_{\pm} decreases with increasing N . At larger N we use the Monte Carlo integrator to evaluate $P(\Lambda)$ and a final trapezoidal integration over Λ to evaluate P_{\pm} .

As can be seen, the same general trends already observed in the analytical case can be seen: the probability that a given minimum has $\phi > 0$ decreases with increasing N , and for a constant σ_0 and σ_1 , the probability also decreases for increasing σ_2 .

3.3 Gaussian Approximations to the Integral

For $N > 10$, direct calculation becomes very resource-intensive. We first select the value of the field value ν that maximizes the integral in in Eq. 2.12, then approximate the integral as a Gaussian integral about that point:

$$\begin{aligned}
N &= A \int_{\lambda_1 \geq \lambda_2 \geq \lambda_3 \dots \geq 0} F \times e^{-Q} dx dy dz \dots \\
&= A \int_{\lambda_1 \geq \lambda_2 \geq \lambda_3 \dots \geq 0} e^{\log F - Q} dx dy dz \dots \\
&\approx \int_{-\infty}^{\infty} e^{-\frac{1}{2} x H x} d^n x = \sqrt{\frac{(2\pi)^n}{\det H}}
\end{aligned}$$

where H is the Hessian at the point being considered, and we no longer have an integral over ν . This approximate value can then be compared against the exact value. The Gaussian approximation turns out to be very good (see Fig. 4). The Gaussian integral can be more efficiently computed than Eq. 2.12, which lets us evaluate it up to $N = 22$.

[LL: Debating putting this up to $N = 35$ or possibly even higher. Where do we stop?]

The plot of the logarithms of these results against the number of dimensions is surprisingly straight (Fig. 5). If we assume that the results can be extrapolated to higher dimensions,⁵ then the value of σ_2 for which $P(F > 0|min)$ drops to $\sim 10^{-500}$ at $N = 100$ is about 1.08. In other words, there will be plenty of minima in the landscape that could correspond to our universe if the landscape has $\sigma_2 \gtrsim 1.08$ (with σ_0 and σ_1 normalized to 1).

4 Implications for Multiverse Cosmology

[RE: I would move from looking at the abstract problem in the previous section to the specific implications for cosmology in this section; and how $P(\Lambda)$ depends on σ_2]

[LL: Dunno what to put here anymore]

5 Conclusion

We have presented results for the statistics of stationary points at a given function value as a function of N and σ_2 . The numbers confirm the intuitive expectation that the probability of a given extremum with $F > 0$ being a minimum decreases as N increases or as σ_2 decreases. We are able to calculate precise values for the probability up to $N = 10$. Above this dimension, evaluating Eq. 2.12 is computationally prohibitive, but we find that Eq. 2.12 is well-approximated by a Gaussian integral. Using this approximation, we are able to estimate the probability up to $N \approx 30$. The results are well-approximated by a straight line when plotted on a logarithmic scale for various values of σ_2 (Fig. 5). If this trend holds to larger values of N , we estimate that the value of σ_2 for which $P(F > 0|min)$ drops to $\sim 10^{-500}$ is approximately 1.08.

The results of this paper establish the number of vacua that could correspond to our universe in string theory, but does not treat the distribution of eigenvalues – and accordingly the duration of slow-roll inflation – that could arise from these vacua. We will save an analysis of this for future work.

⁵Per Figure 4 of [21], this assumption might not hold, especially for $N > 100$.

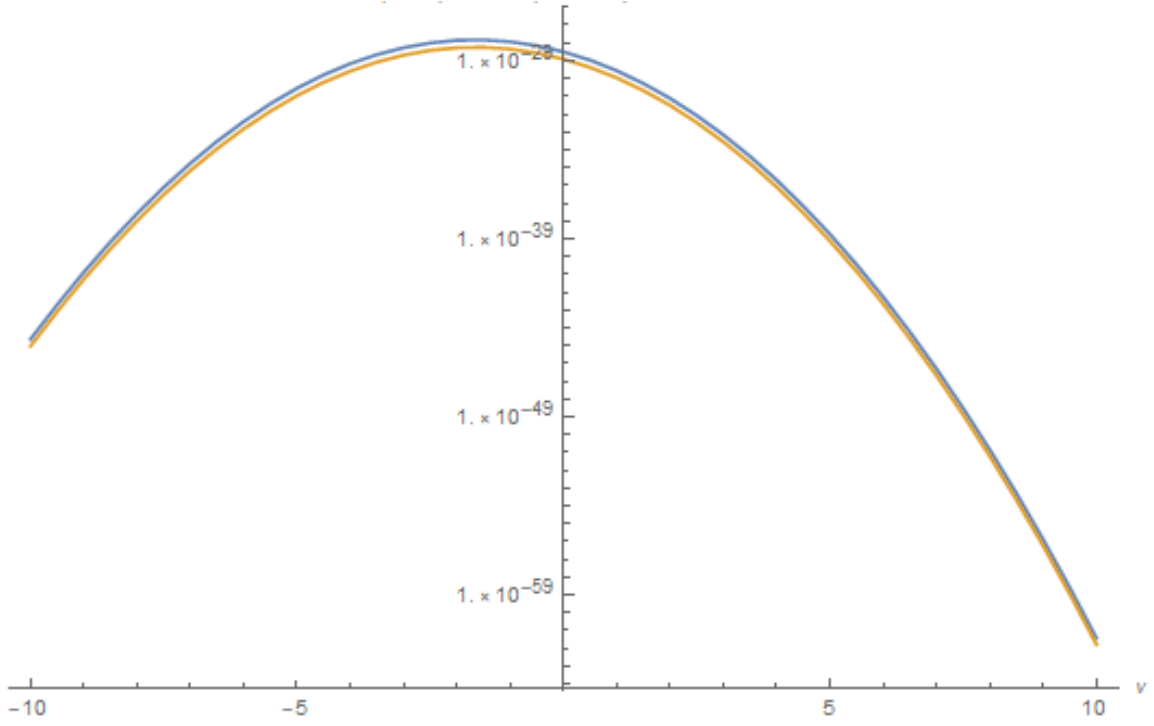


Figure 4. A comparison of the exact integral of Eq. 2.12 with the Gaussian approximation, at specified values of ν ($N = 8$). Blue line corresponds to the Gaussian results, while the orange line corresponds to the exact integral. Horizontal axis is ν while the vertical axis is (unnormalized) likelihood. As expected, because the Gaussian integral integrates to infinity while the exact integral does not, it yields a larger likelihood.

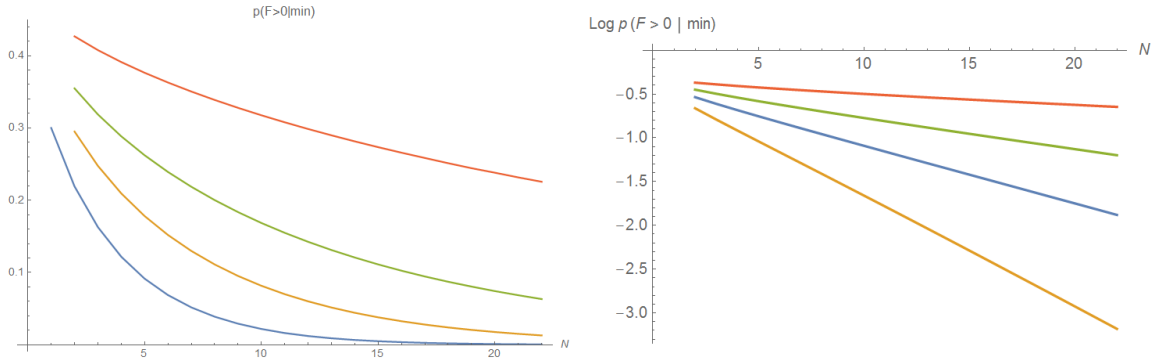


Figure 5. (Left) The probability of a minimum above $\nu = 0$, calculated using the Gaussian approximation. The lines correspond to $\gamma = \frac{1}{10}, \frac{1}{5}, \frac{1}{3.5}, \frac{1}{2.5}$ respectively from top to bottom. Compare Fig. 3. (Right) The same data, plotted using a different y-axis (Log here is to base 10). All four lines yield a logarithm well above -500 at $N = 100$. The cutoff at which $p(F > 0 | \min) \sim 10^{-500}$, with σ_0 and σ_1 normalized to 1, is $\sigma_2 \approx 1.08$.

6 Appendix

6.1 Density of peaks for $N = 4$

For $N = 4$, the full result of the integral Eq. 2.12 is:

$$N = \frac{1}{214990848} \text{Exp} \frac{9x^2\sigma_1^4 + 2\nu x\sigma_0\sigma_1^2\sigma_2 - (v^2 + 10x^2)\sigma_0^2\sigma_2^2}{-2\sigma_1^4 + 2\sigma_0^2\sigma_2^2} \left(80x - 1610e^{3x^2} + 128x^3 + 418e^{3x^2}x^3 + 4e^{4x^2}\sqrt{\pi}(3 + 48x^2 + 64x^4)\text{Erf}\left[\sqrt{\frac{3}{2}}x\right] \right. \\ \left. - 486e^{\frac{9x^2}{2}}\sqrt{6\pi}x^2\text{Erf}\left[\sqrt{\frac{3}{2}}x\right] + 81e^{\frac{9x^2}{2}}\sqrt{6\pi}x^4\text{Erf}\left[\sqrt{\frac{3}{2}}x\right] \right) \quad (6.1)$$

The higher-dimensional results take the same form: an overall exponential multiplied by a product of polynomials and error functions; however they are massive (for 5D for example, there are some eight hundred terms).

6.2 $p(F|s.p.)$ for $N = 2$

The full expression for $p(F|s.p.)$ in 2D is:

$$p(F|s.p.) = \frac{\sqrt{\pi}}{4\sqrt{4\gamma^2 - 6}} \left[\text{Exp} \frac{\nu^2}{2(\gamma^2 - 1)} \left(2\text{Exp} \left(\frac{\nu^2\gamma^2}{e^6 - 10\gamma^2 + 4\gamma^4} \right) \sqrt{\gamma^2 - 1} \right. \right. \\ \left. \left. - \text{Exp} \left(\frac{\nu^2\gamma^2}{2 - 2\gamma^2} \right) (\nu^2 - 1)(\gamma^2 - 1)\gamma^2 \sqrt{\frac{2\gamma^2 - 3}{1 - \gamma^2}} \right) \right] \quad (6.2)$$

where $\gamma = \sigma_1^2/\sigma_0\sigma_2$. This result can be derived using a similar method as to derive Eq. 2.12, but by relaxing the requirement that the smallest eigenvalue is greater than zero.

References

- [1] Planck Collaboration 2018 results. Submitted to *Astronomy & Astrophysics*.
- [2] Dark Energy Survey year 1 results. arXiv:1802.05257
- [3] A. D. Linde, Phys. Lett. B 175, 4, 395–400, 1986
- [4] P. Adshead, R. Easther, and E. A. Lim, Phys. Rev. D 79, 063504, 2009
- [5] A. Guth, arXiv: astro-ph/0101507
- [6] L. Susskind, arXiv:hep-th/0302219
- [7] R. Bousso and J. Polchinski, Journal of High Energy Physics, 06, 006, 2000
- [8] P. Agrawal, G. Obied, P. J. Steinhardt, C. Vafa, Physics Letters B, 784, 271–276, 2018
- [9] A. Masoumi, A. Vilenkin and M. Yamada, Journal of Cosmology and Astroparticle Physics, 05:053, 2017

- [10] A. Masoumi, A. Vilenkin and M. Yamada, *Journal of Cosmology and Astroparticle Physics*, 12:035, 2017
- [11] T. Bjorkmo and M.C.D. Marsh, *Journal of Cosmology and Astroparticle Physics*, 02:037, 2018
- [12] A. Aazami and R. Easther, *Journal of Cosmology and Astroparticle Physics* (0603:013), 2006
- [13] A. J. Bray and D. S. Dean, *Physical Review Letters*, 98, 150201, 2007
- [14] R. Easther and L. McAllister, *Journal of Cosmology and Astroparticle Physics* 05:018, 2006
- [15] J. Frazer and A. R. Liddle, *Journal of Cosmology and Astroparticle Physics* 02:026, 2011
- [16] S.-H. Henry Tye, J. J. Xu and Y. Zhang, *Journal of Cosmology and Astroparticle Physics* 04:018, 2009
- [17] M.C.D. Marsh, L. McAllister, E. Pajer and T. Wrase, *Journal of Cosmology and Astroparticle Physics* 11:040, 2013
- [18] N. Agarwal, R. Bean, L. McAllister and G. Xu, *Journal of Cosmology and Astroparticle Physics* 09:002, 2011
- [19] I.S. Yang, *Physical Review D*, 86, 103537, 2012
- [20] A. Masoumi and A. Vilenkin, *Journal of Cosmology and Astroparticle Physics* 03:054, 2016
- [21] M. Yamada and A. Vilenkin, *Journal of High Energy Physics* 2018: 29, 2018
- [22] Y. V. Fyodorov, *Physical Review Letters*, 92, 240601, 2004
- [23] M. R. Douglas, B. Shiffman and S. Zelditch, *Communications in Mathematical Physics*, 252, 325, 2004
- [24] M. R. Douglas, B. Shiffman and S. Zelditch, *Communications in Mathematical Physics*, 265, 617, 2006
- [25] Y. V. Fyodorov and I. Williams, *Journal of Statistical Physics*, 129, 5, 2007
- [26] Y. V. Fyodorov and C. Nadal, *Physical Review Letters*, 109, 167203, 2012
- [27] Y. V. Fyodorov, P. L. Doussal, A. Rosso, C. Texier, *Annals of Physics*, 397, 2018
- [28] V. Ros, G. B. Arous, G. Biroli and C. Cammarota, *Physical Review X* 9, 011003
- [29] D. S. Dean and S. N. Majumdar, *Physical Review E*, 77, 041108, 2008
- [30] S. N. Majumdar, C. Nadal, A. Scardicchio, and P. Vivo., *Physical Review Letters*, 103, 220603, 2009
- [31] T.C. Bachlechner, *Journal of High Energy Physics*, 2014: 54, 2014
- [32] D. Battefeld, T. Battefeld, S. Schulz, *Journal of Cosmology and Astroparticle Physics*, 06:034, 2012
- [33] Y. V. Fyodorov, *Markov Processes Relat. Fields*, 21, 483–51, 2015

- [34] A. Masoumi, M. Yamada and A. Vilenkin, *Journal of Cosmology and Astroparticle Physics*, 07:003, 2017
- [35] R. Easther, A. Guth and A. Masoumi, arXiv:1612.05224 (2016)
- [36] M. Kac, *Bull. Amer. Math. Soc.*, 43, 314–320, 1943
- [37] S. O. Rice, *Bell System Tech. J.*, 24, 46–156, 1945
- [38] J. M. Bardeen, J. R. Bond, N. Kaiser, and A. S. Szalay, *Astrophysical Journal*, *Astrophysical Journal*, vol. 304, page 15-61 (1986)
- [39] See e.g. H. Goldstein, C. P. Poole, and J. L. Safko, *Classical Mechanics 3rd ed.*, Pearson (2001)
- [40] G. P. Lepage, *Journal of Computational Physics* 27, 192, 1978.
- [41] B. Gough, *GNU Scientific Library Reference Manual - Third Edition, 3rd ed.* (Network Theory Ltd., 2009).
- [42] M. R. Douglas, *Journal of High Energy Physics*, 05:046, 2003